Published in final edited form as:
J Struct Funct Genomics. 2009 April ; 10(2): 157–163. doi:10.1007/s10969-008-9052-9.

Crystal structure of fatty acid/phospholipid synthesis protein PlsX from *Enterococcus faecalis*

Y. Kim, **H. Li**, **T. A. Binkowski**, **D. Holzle**, and **A. Joachimiak**
Midwest Center for Structural Genomics and Structural Biology Center, Biosciences, Argonne National Laboratory, 9700 South Cass Ave., Bldg 202, Argonne, IL 60439, USA

Y. Kim: ; H. Li: ; T. A. Binkowski: ; D. Holzle: ; A. Joachimiak: andrzejj@anl.gov

Abstract

PlsX is a key enzyme that coordinates the production of fatty acids and membrane phospholipids. The *plsX* gene is co-localized with a bacterial *fab* gene cluster which encodes several key fatty acid biosynthetic enzymes. The protein is a member of a large, conserved protein family (Pfam02504) found exclusively in bacteria. The PlsX sequence homologues include both phosphate acetyltransferases and phosphate butaryltransferases that catalyze the transfer of an acetyl or butaryl group to orthophosphate. We have determined the crystal structure of PlsX from the human pathogen *Enterococcus faecalis*. PlsX is a $\alpha/\beta/\alpha$ sandwich that resembles a Rossmann fold and forms a dimer. A putative catalytic site has been identified within a deep groove on the interface between monomers. This site showed strong surface similarity to epimerases and reductases. It was recently proposed that PlsX is a phosphate acyltransferase that catalyzes the formation of acyl-phosphate from the acyl–acyl carrier protein; however the specific biochemical function of the PlsX protein awaits further experimental scrutiny.

Keywords

Rossmann fold; Fatty acid/phospholipid synthesis

Introduction

Enterococcus faecalis, a Gram-positive bacterium, is a natural inhabitant of the mammalian gastrointestinal tract and is found in soil, sewage, water and food, frequently through fecal contamination. It is an opportunistic pathogen that is a major cause of urinary tract infections, bacteremia, and infective endocarditis [1]. A further understanding of *E. faecalis* is important in human healthcare, as it has developed resistance to the strongest known antibiotics.

The crystal structure of PlsX, a predicted fatty acid/phospholipid synthesis protein from *E. faecalis*, has been determined and refined to 2.26 Å using the single wavelength anomalous diffraction (SAD) method. The protein belongs to a large protein family (over 2500 members) found exclusively in bacteria [2]. The PlsX sequence homologues belong to Pfam02504—PlsX protein family that has been associated with fatty acid synthesis, and Pfam01515—this family

Correspondence to: A. Joachimiak, andrzejj@anl.gov.

includes both phosphate acetyltransferases and phosphate butaryltransferases, that catalyze the transfer of an acetyl or butaryl group to orthophosphate. The *plsX* gene is co-localized with bacterial *fab* gene cluster which encodes several key fatty acid biosynthetic enzymes. In *Escherichia coli* the PlsX protein is required for glycerol-3-phosphate auxotrophy.

Materials and methods

Cloning, protein purification and crystallization

The ORF of the *E. faecalis* fatty acid/phospholipid synthesis PlsX protein was amplified from genomic DNA with *KOD* DNA polymerase using conditions and reagents provided by the vendor (Novagen, Madison, WI). The gene was cloned into a pMCSG7 vector [3] using a modified ligation independent cloning protocol [4]. This process generated an expression clone producing a fusion protein with an N-terminal His_6 tag and a TEV protease recognition site (ENLYFQ↓S). The fusion protein was overproduced in *E. coli* BL21-derivative harboring a plasmid encoding three rare *E. coli* tRNAs (Arg [AGG/AGA] and Ile [ATA]). A selenomethionine (SeMet) derivative of the expressed protein was prepared as described by Walsh et al. [5]. The protein was purified by resuspension of IPTG-induced bacterial cells in binding buffer (500 mM NaCl, 5% glycerol, 100 mM HEPES, pH 8.0, 10 mM imidazole, and 10 mM β-mercaptoethanol). The cells were lysed by the addition of lysozyme to 1 mg/ml in the presence of a protease inhibitor mixture cocktail (Sigma P8849) (0.25 ml/5 g cells) and sonication for 2–3 min. After clarification by centrifugation (30 min at 30,000*g*) and passage through a 0.2 μm filter, the lysate was applied to Ni-NTA Superflow resin (Qiagen) and unbound proteins were removed by washing with five volumes of binding buffer. The protein was eluted from the column with 250 mM imidazole, and the fusion tag was cleaved with recombinant His-tagged TEV protease [6]. Native protein was purified from the His tag, undigested protein and TEV protease by application of the solution to a second Ni-NTA column. The PlsX protein was dialyzed against 10 mM HEPES pH 7.5, 500 mM NaCl, and concentrated using a BioMax concentrator (Millipore). Before crystallization, any particulate matter was removed from the sample by passage through a 0.2 μm Ultrafree-MC centrifugal filtration device (Millipore, Inc., Bedford, MA).

Protein crystallization

The protein was crystallized by vapor diffusion in hanging drops by mixing 1 μl of the protein solution (15 mg/ml) with 1 μl of 0.1 M HEPES pH 7.5, 15% Ethanol, 0.2 M $MgCl_2$, and equilibrated at 295 K over 500 μl of this solution. Crystals, which appeared after 24 h, were flash-cooled in liquid nitrogen with crystallization solution plus 15% glycerol as cryoprotectant prior to data collection. The crystals belong to the orthorhombic space group $P2_12_12_1$ with unit cell dimensions of a = 62.36 Å, b = 82.42 Å, c = 147.24 Å, $\alpha = \beta = \gamma = 90°$.

Data collection

Diffraction data were collected at 100 K at the 19ID beamline of the Structural Biology Center at the Advanced Photon Source, Argonne National Laboratory. The single wavelength SAD data up to 2.26 Å near the selenium peak energy (12.658 keV; 0.9793 Å) were collected using inverse-beam strategy from a SeMet-labeled protein crystal. One crystal (0.2 × 0.2 × 0.2 mm) was used to collect data at 100 K. All SAD data sets were collected with 8 s exposure/2.0°/frame (rotation of ω) using 225 mm crystal to detector distance. The total oscillation range covered 280° in ω, 140° were with φ = 0 and the other 140° with φ = 180, which was 30° more than a suggested range predicted by the strategy module of HKL2000 [7]. All data were processed and scaled with HKL2000 to an Rmerge of 12.7% (Table 1).

Structure determination and refinement

The structure was determined by SAD phasing using HKL2000_PH, SHELXC, SHELXD, SHELXE, MLP-HARE, SOLVE/RESOLVE [8] and refined at 2.26 Å using REFMAC [8] against the peak data. The initial partial model was autotraced using RESOLVE [9] and more residues were added using ARP/wARP [10]. Manual addition of residues and adjustment using COOT [8] were required to complete the model for refinement. Several rounds of manual adjustments using COOT and REFMAC refinements were done to converge the model with the final R 20.9% and the free R of 26.2% (Table 2). Electron density calculated at 1.0 σ is well connected for the most of the main chain except a region of residues 1–10 which are disordered in the crystal structure. The stereochemistry of the structure was validated with PROCHECK [11] and the Ramachandran plot. The main chain torsion angles for all residues are in the allowed regions or additional allowed regions. In addition to 307 waters, one molecule of ethylene glycol and four ethanol molecules were modeled in the structure.

Data deposition

Atomic coordinates of PlsX have been deposited into the PDB as 1U7 N.

Discussion

PlsX monomer is an $\alpha/\beta/\alpha$ sandwich and belongs to a Rossmann fold (Fig. 1). The twisted β-sheet has 11 mostly parallel strands that are arranged in the order $\beta3$ $\beta2$ $\beta1$ $\beta4$ $\beta11$ $\beta10$ $\beta5$ $\beta6$ $\beta9$ $\beta7$ $\beta8$. The sheet is flanked by 13 helices: $\alpha1$, $\alpha2$, $\alpha8$, $\alpha9$, $\alpha10$, $\alpha11$ and $\alpha12$ on one side and $\alpha3$, $\alpha4$, $\alpha5$, $\alpha6$, $\alpha7$ and $\alpha13$ on the other side of the sheet. The monomer has a well defined hydrophobic core and the structure is stabilized by a number of intra-subunit salt bridges on the protein surface (Lys25/Asp48, Lys43/Glu39, Lys44/Glu41, Lys74/Asp65, Arg167/Asp137, Arg173/Asp220, Lys192/Glu195, Lys280/Asp277, Arg306/Arg310/Asp27). The PlsX protein forms an S-shaped dimer using the novel dimerization motif (Fig. 1). Two α-helices $\alpha9$ and $\alpha10$ form a long hairpin in each monomer that protrudes away from the main domain. The hairpins associate and form a four-helix bundle ($\alpha9$, $\alpha10$ and $\alpha9'$, $\alpha10'$) with a well defined hydrophobic core. The loop between helices $\alpha9$ and $\alpha10$ is disordered in the crystal. In the *E. faecalis* PlsX protein, the base of this four-helix bundle includes 12 methionine residues (Met129, Met241, Met243, Met244, Met272 and Met276 and symmetry mates) that interact through Van der Waals contacts and form a rather unusual methionine belt (Fig. 1b). The dimer is additionally stabilized by the interaction of the loops and α-helices of the main domain.

Primary sequence and secondary structure analysis

The PlsX has two sequence homologues in the Protein Data Bank (PDB). The FASTA search [12] found a PlsX-like protein from *Bacillus subtilis* (PDB ID = 1VIL) with 50.6% sequence identity and the MoeA protein involved in molybdopterin biosynthesis from *Pyrococcus horikosii* (PDB id = 1UZ5) with 25.6% sequence identity. The secondary structure matching program (SSM) identified several structural homologues. The top matches include: a PlsX-like protein from *B. subtilis*—fatty acid/phospholipid synthesis protein (PDB ID = 1VIL), and several phosphotransacetylases from *B. subtilis* (PDB ID = 1XCO and 1TD9), *Methanosarcina thermophila* (PDB ID = 1QZT), and *Streptococcus pyogenes* (PDB ID = 1R5 J). The PlsX sequence produced no matching motifs to the superfamily HMM library.

Putative active site

Between the dimerization and the main domain there is a deep groove formed by several secondary structure elements ($\beta5$, $\beta10$, $\beta11$, $\alpha3$, $\alpha5$, $\alpha9$, $\alpha11$) and several connecting loops. Analysis of the groove by CASTp (surface ID = 68, chain A) reveals 114 residues forming a

solvent accessible surface with area and volume of 1,763 Å^2 and 1,870 Å^3, respectively [13]. The surface is highlighted in Fig. 2a (yellow). The number of residues on the edges of this groove is highly conserved (including Asp277, Tyr278, Ser279, Lys295 and His297 residues (Fig. 3)) and also contains several hydrophobic residues at the bottom of the cleft. Further CASTp analysis, using a smaller probe radius to exclude domain interface regions, revealed two well defined subpockets within the large cleft (Fig. 2a). The smaller subpocket (CASTp ID = 34, chain J) (Fig. 2a, cyan) contains 32 residues and has a solvent accessible area and volume of 303 Å^2 and 130 Å^3, respectively. The larger subpocket (CASTp ID = 35, chain J) (Fig. 3a, orange) contains 40 residues and has a solvent accessible area and volume of 535 Å^2 and 531 Å^3, respectively. These pocket sites may represent the active/catalytic site of the protein.

Surface analysis

In attempt to identify potential substrates, the putative functional surfaces were submitted to the pvSOAR server for comparison to known ligand binding surfaces [14]. The best surface matches to the larger subpocket (CASTp ID = 35, chain J) (Fig. 2a, orange) came from enzymes binding cofactors: nicotinamide adenosine dinucleotide phosphate (NADP) and coenzyme A (CoA). In both cases, the coenzymes adopted an open conformation spanning approximately 15 Å with the adenosine base and ribose 2′ phosphate group in similar conformations (Fig. 2b–d). The surface walls around the dinucleotide diphosphate bridge are conserved by a grouping of Asp, Glu, Ser, Thr, and Gly which is conserved in PlsX.

The best hit containing an NADP cofactor was ADP-L-glycero-D-mannoheptose 6-epimerase (AGME) from *E. coli* (PDB ID = 1EQ2, E.C.5.1.3.20). AGME is an enzyme required for lipopolysaccharide (LPS) biosynthesis in most genera of pathogenic and non-pathogenic Gram-negative bacteria, catalyzing the interconversion between ADP-D-glycero-D-mannoheptose and ADP-L-glycero-D-mannoheptose [15]. AGME is classified as a member of the short chain dehydrogenase/reductase (SDR) superfamily, containing the conserved catalytic triad Ser116-Tyr140-Lys144. The putative functional surface of PlsX shares 19 conserved residues with the NADP binding surface of AGME (CASTp ID = 33, chain J) (Fig. 2b). The conserved residues superimpose with a cRMSD and oRMSD *P*-values of 6.4×10^{-3} and 1.8×10^{-5}, respectively. These residues include the SRD catalytic triad (Ser279-Tyr278-Lys295). Of the 19 conserved residues, 12 have been identified as potential hydrogen bonding residues in AGME [15]. Overall, the surfaces have a similar solvent accessible surface (835 and 923 Å^2) and volume (1480 and 1449 Å^3) for PlsX and AGME, respectively. NADP from AGME has been modeled into the corresponding pocket in PlsX the pocket based on the superposition of the conserved residues (Fig. 2e, orange).

PlsX also showed strong surface similarity to GDP-4-keto-6-deoxy-D-mannose epimerase/reductase (GMER) from *E. coli* (PDB ID = 1BWS, E.C.1.1.1.271). GMER is a member of the reductase-epimerase-dehydrogenase (RED) enzyme superfamily to which the SDRs also belong [16]. The NADP binding surface (CASTp ID = 35) shares 18 conserved residues including the catalytic triad (Ser107-Tyr136-Lys140) with PlsX (Fig. 2c). The conserved residues superimpose with a cRMSD and oRMSD *P*-values of 7.4×10^{-3} and 3.8×10^{-6}, respectively. The coenzyme is bound in a similar conformation to that of bound AGME (Fig. 2c). The NADP binding surfaces in AGME and GMER both have a well defined surface directly adjacent to them, similar to the subpocket of PlsX. In AGME, the ADP-glucose binding site is located adjacent to the to NADP binding site (Fig. 2b, cyan). In GMER, the substrate GDP-L-fucose complex was modeled into a well defined pocket adjoining the NADP surface (Fig. 2c, cyan). The smaller subpocket (CASTp ID = 34, chain J) (Fig. 2a, cyan) was searched against known nucleotide binding surfaces. ADP binding surfaces were the best scoring nucleotide, with the adenine base oriented away from the NADP binding surface and the

diphosphate directly toward it. The ADP binding surface of homoserine kinase (PDB ID = 1FWK, E.C.2.7.1.39) from *M. jannashii* shared 15 conserved residues superimpose with a cRMSD and oRMSD *P*-values of 4.3×10^{-4} and 1.8×10^{-8}, respectively. This ADP structure has been modeled in the pocket in Fig. 2e (cyan) based on the superposition of the conserved residues. Therefore, it is possible that a ligand containing ADP could bind adjacent to the NADP binding site in PlsX, similar to that seen in AGME and GMER.

Interestingly PlsX larger subpocket shows also surface similarity to proteins binding CoA coenzymes (CASTp ID = 35) (Fig. 2a, orange). While the ADP portions of CoA were all in similar orientations in the high scoring hits, the pantothenic arm was found in a variety of conformations, affecting the overall superposition of the conserved residues. The most significant hits were when the CoA was in fully extended conformation as seen in carnitine acyltransferase (CRAT) from *M. musculus* (PDB ID = 1NDI, E.C.2.3.1.7) (Fig. 2d, orange). CRAT, an important enzyme in fatty acid transport, catalyzes the exchange of acyl groups between carnitine and CoA through a catalytic His343 residue [17]. The active site is composed of two separate channels created at a deep grove formed by the N and C domain interface (Fig. 2d). The catalytic His residue lies at the intersection of the two pockets. The putative functional surface of PlsX shares 19 conserved residues with the CoA-binding surface of CRAT. The conserved residues superimpose with a cRMSD and oRMSD *P*-values of 5.3×10^{-3} and 1.9×10^{-8}, respectively. However, the equivalent catalytic His281 residue is not conserved in PlsX family.

Genomic analysis

Although the specific biochemical function of the PlsX protein awaits experimental scrutiny, additional cellular functional information can be inferred from genomic localization and gene coexpression. The analysis of the *fab* gene cluster shows that in many bacterial genomes the *plsX* gene is located next to *acpP* that codes for acyl carrier protein—a key protein cofactor in fatty acid synthesis. The analysis of transcription of *fab* gene cluster shows obligatory co-transcription of pairs of genes required for normal growth with a promoter located immediately upstream of the coding sequence. It was shown by Podkovyrov and Larson [18] that *plsX* and *rpmF* are co-transcribed. *rpmF* codes for ribosomal protein L32, suggesting that the expression of lipid and ribosome biosynthetic genes may be coordinated. If *rpmF-plsX* co-transcription is functionally important, disruption of this coordinated expression might be expected to slow or block bacterial growth under certain conditions. However, this conclusion is tempered by the lack of information about the specific biochemical function of the PlsX protein.

The PlsX has been also linked to the glycerol-3-phosphate pathway. It was shown that mutations in *E. coli plsB* and *plsX* genes are required for sn-glycerol-3-phosphate auxotrophy [19]. The *plsX* mutation (*plsX*50) has been reported to be a single-base pair deletion upstream of the coding sequence (GenBank accession no. M96793), and it is unclear whether this mutation causes a gain of function or a loss of function relative to the wild-type gene, since no complementation studies have been reported. *plsB* codes for the sn-glycerol-3-phosphate acetyltransferase suggesting that *plsX* function is somehow, directly or indirectly, linked to glycerol-3-phosphate pathway.

Most bacterial genomes sequenced to date encode a PlsX homologue, and thus, this protein seems likely to play an important role in cellular physiology. The crystal structure suggests that the PlsX may be an enzyme utilizing NADP and using substrate containing a nucleotide module. The possibility that the proposed active site of PlsX could accommodate both NADP and CoA is very intriguing and may suggest an evolutionary relationship between PlsX and CoA-binding proteins (although the potential catalytic His281 residue is not conserved in PlsX) as well as NADP binding proteins (the potential catalytic Ser279-Tyr278-Lys295 motif is highly conserved). There is also prospect that in some species PlsX may play dual functions.

It was reported recently that PlsX in *B. subtilis* is acyl–acyl carrier protein [ACP]:phosphate acyltransferase that catalyzes the formation of acyl-phosphate (acyl-PO_4) from acyl-ACP [20]. Moreover the depletion of PlsX led to the cessation of both fatty acid synthesis and phospholipid synthesis. These data suggest that PlsX is a key enzyme that coordinates the production of fatty acids and membrane phospholipids in *B. subtilis*. It was also reported that both *plsX* and *yneS* genes are essential for acyl-phosphate synthesis in *B. subtilis* and *E. coli* cells lacking *plsB* gene. Therefore it appears that *plsX* and *yneS* genes play important roles in bacterial growth, possibly by regulating the intracellular concentration of acyl-ACP [21]. Further functional validation experiments will enable a better understanding of PlsX function.

Acknowledgments

We wish to thank all members of the Structural Biology Center at Argonne National Laboratory for their help in conducting experiments. This work was supported by National Institutes of Health Grant GM62414, GM074942 and by the U.S. Department of Energy, Office of Biological and Environmental Research, under contract DE-AC02-06CH11357.

References

1. Paulsen IT, et al. Role of mobile DNA in the evolution of vancomycin-resistant *Enterococcus faecalis*. Science 2003;299:2071–2074. [PubMed: 12663927]
2. Altschul SF, Madden TL, Schaffer AA, Zhang J, Zhang Z, Miller W, Lipman DJ. Gapped BLAST and PSI-BLAST: a new generation of protein database search programs. Nucleic Acids Res 1997;25(17): 3389–3402. [PubMed: 9254694]
3. Stols L, Gu M, Dieckman L, Raffen R, Collart FR, Donnelley MI. A new vector for high-throughput, ligation-independent cloning encoding a tobacco etch virus protease clevage site. Protein Expr Purif 2002;25:8–15. [PubMed: 12071693]
4. Dieckman L, Gu M, Stols L, Donnelley MI, Collart FR. Protein Expr Purif 2002;25:1–7. [PubMed: 12071692]
5. Walsh MA, Dementieva I, Evans G, Sanishvili R, Joachimiak A. Taking MAD to the extreme: ultrafast protein structure determination. Acta Crystallogr D Biol Crystallogr 1999;55:1168–1173. [PubMed: 10329779]
6. Kim Y, Dementieva I, Zhou M, Wu R, Lezondra L, Quartey P, Joachimiak G, Korolev O, Li H, Joachimiak A. Automation of protein purification for structural genomics. J Struct Funct Genomics 2004;5:111–118. [PubMed: 15263850]
7. Brunger AT, Adams PD, Clore GM, DeLano WL, Gros P, Grosse-Kunstleve RW, Jiang JS, Kuszewski J, Nilges M, Pannu NS, Read RJ, Rice LM, Simonson T, Warren GL. Crystallography & NMR system: a new software suite for macromolecular structure determination. Acta Crystallogr D Biol Crystallogr 1998;54:905–921. [PubMed: 9757107]
8. Collaborative Computational Project, Number 4. The CCP4 suite: programs for protein crystallography. Acta Crystallogr D Biol Crystallogr 1994;50:760–763. [PubMed: 15299374]
9. Terwilliger TC. SOLVE and RESOLVE: automated structure solution and density modification. Methods Enzymol 2003;374:22–37. [PubMed: 14696367]
10. Morris RJ, Perrakis A, Lamzin VS. ARP/wARP and automatic interpretation of protein electron density maps. Methods Enzymol 2003;374:229–244. [PubMed: 14696376]
11. Laskowski RA, MacArthur MW, Moss DS, Thornton JM. PROCHECK: a program to check the stereochemical quality of protein structures. J Appl Cryst 1993;26:283–291.
12. Pearson WR. Flexible sequence similarity searching with the FASTA3 program package. Methods Mol Biol 2000;132:185–219. [PubMed: 10547837]
13. Binkowski TA, Naghibzadeh S, Liang J. CASTp: computed atlas of surface topography of proteins. Nucleic Acids Res 2003;31:3352–3355. [PubMed: 12824325]
14. Binkowski TA, Freeman P, Liang J. pvSOAR: detecting similar surface patterns of pocket and void surfaces of amino acid residues on proteins. Nucleic Acids Res 2004;32:W555–W558. [PubMed: 15215448]

15. Deacon AM, Ni YS, Coleman WG Jr, Ealick SE. The crystal structure of ADP-L-glycero-D-mannoheptose 6-epimerase: catalysis with a twist. Structure Fold Des 2000;8(5):453–462. [PubMed: 10896473]

16. Rizzi M, Tonetti M, Vigevani P, Sturla L, Bisso A, Flora AD, Bordo D, Bolognesi M. GDP-4-keto-6-deoxy-D-mannose epimerase/reductase from *Escherichia coli*, a key enzyme in the biosynthesis of GDP-L-fucose, displays the structural characteristics of the RED protein homology superfamily. Structure 1998;6(11):1453–1465. [PubMed: 9817848]

17. Jogl G, Tong L. Crystal structure of carnitine acetyltransferase and implications for the catalytic mechanism and fatty acid transport. Cell 2003;112(1):113–122. [PubMed: 12526798]

18. Podkovyrov S, Larson TJ. Lipid biosynthetic genes and a ribosomal protein gene are cotranscribed. FEBS Lett 1995;368:429–431. [PubMed: 7635191]

19. Bernstein BE, Williams DM, Bressi JC, Kuhn P, Gelb MH, Blackburn GM, Hol WG. A bisubstrate analog induces unexpected conformational changes in phosphoglycerate kinase from *Trypanosoma brucei*. J Mol Biol 1998;279:1137–1148. [PubMed: 9642090]

20. Paoletti L, Lu YJ, Schujman GE, de Mendoza D, Rock CO. Coupling of fatty acid and phospholipid synthesis in *Bacillus subtilis*. J Bacteriol 2007;189:5816–5824. [PubMed: 17557823]

21. Yoshimura M, Oshima T, Ogasawara N. Involvement of the YneS/YgiH and PlsX proteins in phospholipid biosynthesis in both *Bacillus subtilis* and *Escherichia coli*. BMC Microbiol 2007;7:69. [PubMed: 17645809]

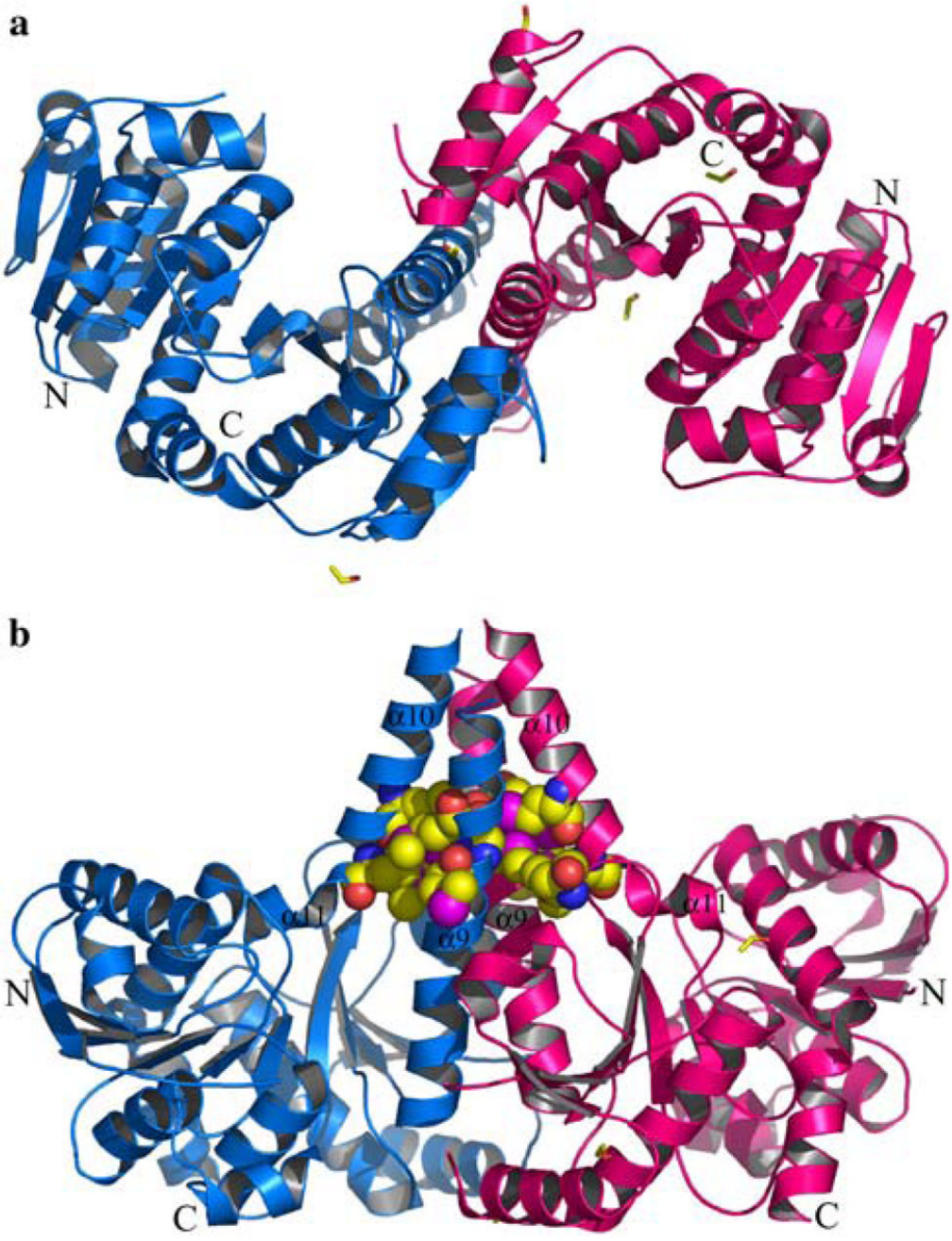

Fig. 1.

Structure of PlsX protein dimer with N- and C- termini labeled. **a** The view is down the two fold axis. One monomer is in blue and second is pink. **b** Orthogonal view in respect to 1a with methionine belt in cpk and helices 9, 10 and 11 labeled

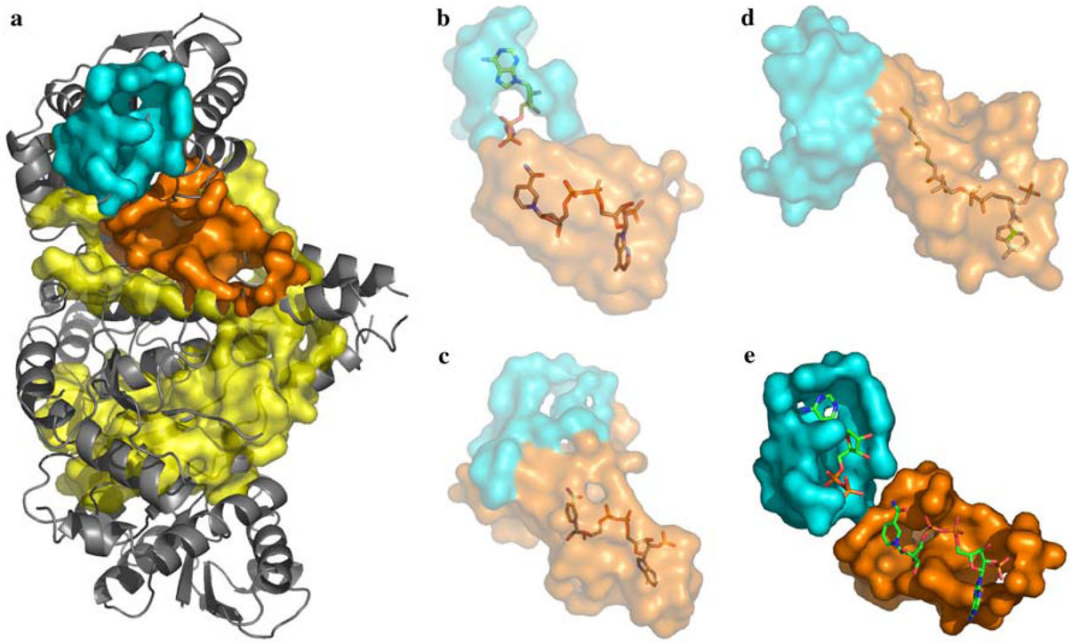

Fig. 2.

The proposed active site surface of PlsX protein is a deep groove (**a**, *yellow*) which contains two conserved subpocket regions (**a**, *cyan and orange*). The NADP (**b**, *orange*) and ADP-glucose (**b**, *cyan*) of ADP-L-glycero-D-mannoheptose 6-epimerase (AGME) from *E. coli* (PDB ID = 1EQ2) and the NADP binding surface (**c**, *orange*) of GDP-4-keto-6-deoxy-D-mannose epimerase/reductase (GMER) from *E. coli* (PDB ID = 1BWS) showed strong similarity to surfaces in PlsX. The CoA (**d**, *orange*) binding surface of carnitine acyltransferase (CRAT) from *M. musculus* (PDB ID = 1NDI) is used to model CoA into the binding surface of PlsX. The coenzymes NADP (**e**, *orange*) and ADP (**d**, *cyan*) have been modeled into PlsX

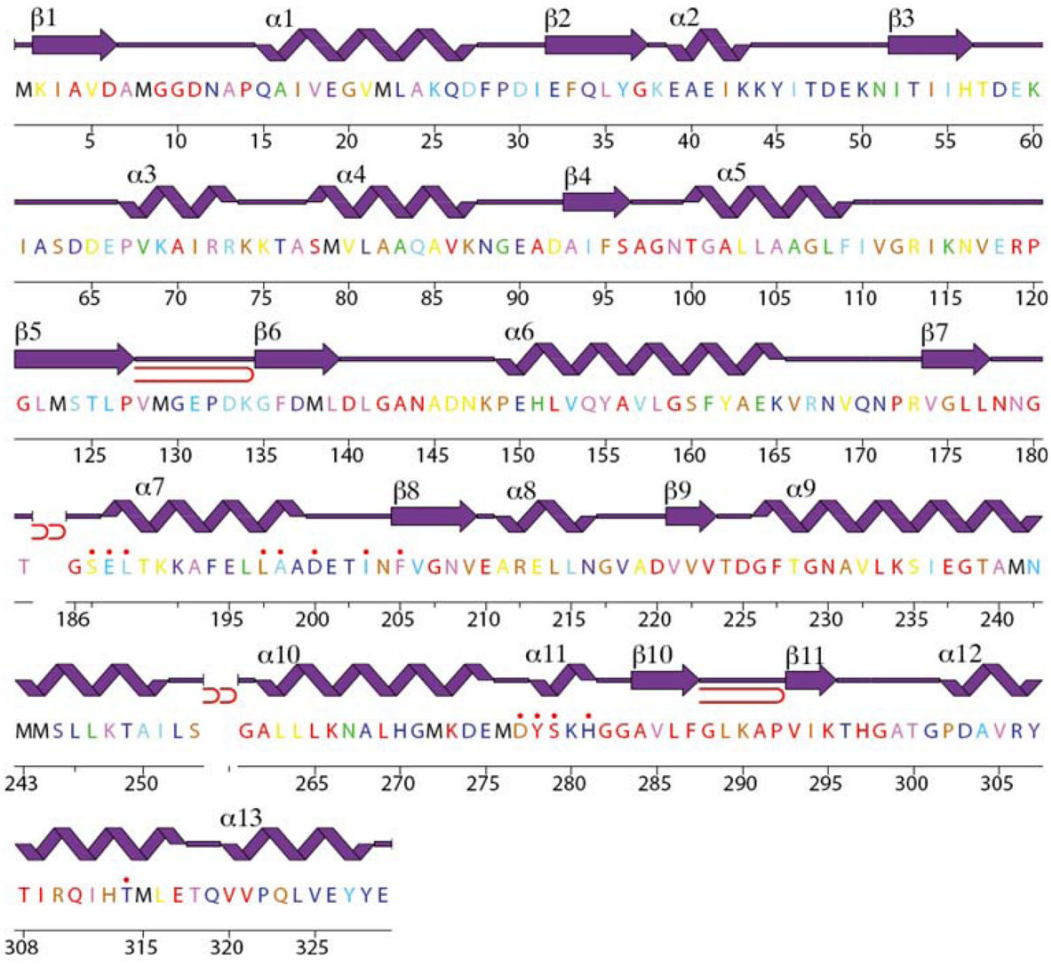

Fig. 3.

Primary sequence aligned with the secondary structure and conservation of residues. The color scale is from black to red, where residues labeled red are the most conserved and residues in black are the least conserved

Table 1

Summary of crystal and SAD data

	SAD data collection
Unit cell	a = 62.36 Å, b = 82.42 Å, c = 147.24 Å, $\alpha = \beta = \gamma$ = 90.00°
Space group	P $2_12_12_1$
MW Da (residues)	36771 (336)
Mol (AU)	2
SeMet (AU)	28

	Peak (Native)
Wavelength (Å)	0.9793
Resolution range (Å)	73.5–2.26 (2.34–2.26)
No. of unique reflections	36201 (3373)
Completeness (%)	99.4 (94.6)
R merge (%)	0.127 (0.64)

Table 2

Crystallographic statistics

Resolution range (Å)	All		
	Number	FOM	Phasing power
Phasing			
50.0–2.26	35818	0.25	1.20
Density modification		0.85	

Refinement	
Resolution range (Å)	73.52–2.26
No. of reflections	34,335
Cutoff	0
R-value (%)	21.0
Free R-value (%)	26.0
Rms deviations from ideal geometry	
Bond length (1–2) (Å)	0.013
Angle (°)	1.443
Dihedral (°)	6.35
No. of atoms	
Protein	4,972
Water	319
Mean B-factor ($Å^2$)	30.7
Ramachandran plot statistics (%)	
Residues in most favored regions	93.1%
Residues in additional allowed regions	6.9%
Residues in disallowed region	0.0%